geoconvention
Calgary • Canada • May 7-11 2018

# Lagrangian Mechanical Model of Porous Rock

*Wubing Deng and Igor B. Morozov*
*University of Saskatchewan, wubing.deng@usask.ca, igor.morozov@usask.ca*

## Summary

Recent seismic-frequency laboratory experiments on attenuation and dispersion in porous sandstone are interpreted by mechanical models of the materials. In contrast to several other methods, we strictly follow the conventional mechanics and construct macroscopic models based on time-and frequency-independent material properties. All material properties (density, elasticity, viscosity, and Darcy pore-flow friction) are described by matrices, which account for fast and slow waves and other poroelastic effects. This property of the model is known as “Biot-consistency”. All types of viscoelastic moduli and other “effective”, frequency-dependent properties are explained as measured (apparent) properties and predicted by the model. The Lagrangian model can also be naturally extended to double porosity, squirt-flow and other wave-induced flow effects, nonlinear viscosity, thermoelasticity, and other physical effects within rock.

## Introduction

Recently, Morozov and Deng (2017) considered the data obtained in low-frequency laboratory and numerical experiments with porous and mesoscopically-heterogeneous rock. Such experiments are usually described either by effective (empirical) viscoelastic (VE) moduli or by micro-mechanical models, most of which are based on local pore-fluid flows (Müller et al., 2010). Such micromechanical models include squirt flows, fluid transport between interconnected pores, wave-induced fluid flows (WIFF) in mesoscopic-scale structures and VE relaxation of pores. Such models examine the effects of certain detailed but greatly simplified microstructures, such as “penny-shaped” planar pores of equal dimensions (e.g., Gurevich et al., 2010), or a network of pores connected by fluid transport (Chapman et al., 2002).

In the present study, we also argue that local pore-fluid flows should be the primary cause of internal friction within porous sandstone, but in contrast to the above approaches, we formulate the model strictly in terms of macroscopic, averaged mechanical properties of the material and assuming no specific microstructure or fluid-flow patterns. Although the microstructures are likely infinitely variable, the significant macroscopic properties should in principle be measurable in the laboratory, similarly to poroelastic moduli and Skempton coefficients in Biot’s (1956) model.

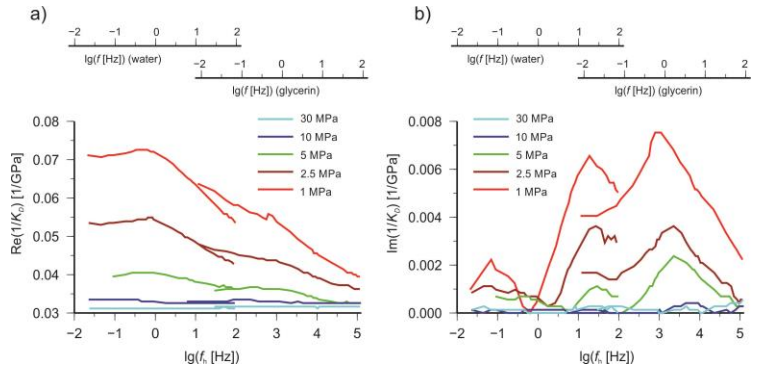


Figure 1. Effective drained bulk compliances $K_D^{-1}$ inverted by Morozov and Deng (2017) from Young’s moduli data by Pimienta et al. (2015), as functions of scaled frequency $f_\eta$: a) real part; b) imaginary part. The scaled frequency is defined as $f_\eta = f\eta/\left(10^{-3}\text{Pa}\cdot\text{s}\right)$, where $\eta$ is the viscosity of saturating fluid. Confining pressures are given in the legends, and types of saturating fluids are shown in the frequency axes along the top of the plots.

The key result by Morozov and Deng (2017) consists in correcting for the effects of the experimental setup and deriving the “true” poroelastic moduli of the sandstone (Figure 1). Most importantly, these properties are not directly obtained in the experiment, and their estimation require mechanical forward modeling and inversion. These

true effective Biot's moduli are represented by frequency-dependent, symmetric 2×2 matrices that can be used to predict the behavior of the material in various types of deformations. However, these effective matrix moduli still need to be explained by true, frequency-independent material properties and time-domain equations governing the deformation of the body. Such determination of the actual material properties is the goal of this paper.

Also in contrast to many existing approaches to modeling dispersion and attenuation effects (including those mentioned above), we formulate the model strictly in terms of conventional, macroscopic continuum mechanics (Landau and Lifshitz, 1986). This formulation means that material properties are time- and frequency-independent, and the dynamics of the rock is described by standard differential equations of mechanics and contain no phenomenological properties such as VE moduli, material memory or extended operators such as Volterra integrals or fractional derivatives in time. This rigorous mechanical model would lead to straightforward numerical implementations for synthetic wavefield modeling and inversion and can be used in all applications ranging from modeling quasi-static pore-fluid flows to predicting the fast and slow wave velocities and reflection coefficients in heterogeneous media.

As a practical application of the approach, in this paper, we derive a macroscopic mechanical model from low-frequency Young's modulus measurements in Fontainebleau sandstone by Pimienta et al. (2015). These data were corrected for experimental effects by Morozov and Deng (2017) (Figure 1).

## Macroscopic Lagrangian description

In Lagrangian form, Biot's (1956) model can be described by giving the following Lagrangian and dissipation functions in a two-dimensional model space of variable $\mathbf{u}$ (Morozov and Deng, 2016a):

$$\begin{cases} L^{\mathrm{B}}\left\{\mathbf{u}\left(\mathbf{x},t\right)\right\} = \frac{1}{2}\dot{\mathbf{u}}_i^T\boldsymbol{\rho}^{\mathrm{B}}\dot{\mathbf{u}}_i - \left(\frac{1}{2}\boldsymbol{\Delta}^T\mathbf{K}^{\mathrm{B}}\boldsymbol{\Delta} + \tilde{\boldsymbol{\varepsilon}}_{ij}^T\boldsymbol{\mu}^{\mathrm{B}}\tilde{\boldsymbol{\varepsilon}}_{ij}\right), \\ D^{\mathrm{B}}\left\{\mathbf{u}\left(\mathbf{x},t\right)\right\} = \frac{1}{2}\dot{\mathbf{u}}_i^T\mathbf{d}\dot{\mathbf{u}}_i. \end{cases} \tag{1}$$

In these expressions, indices $i, j = 1,2,3$ (or $x$,$y$,$z$) denote the spatial coordinates, summations over repeated spatial indices are implied, and matrix (boldface) notation is used with respect to the two-dimensional model space. Six "generalized displacement" describing the displacement of the rock and its pore fluid are combined in a vector $\mathbf{u}$, with components denoted $u_{Ji}$. Vector $u_{1i}$ is the observable displacement of the fluid-saturated rock, and vector $u_{2i}$ denotes the filtration-fluid displacement multiplied by porosity $\phi_J$: $u_{Ji} \equiv -w_{Ji} \equiv -\phi_J\left(u_{\mathrm{fluid}J,i} - u_{1i}\right)$. The model vector combining spatial scalars $\boldsymbol{\Delta} \equiv \boldsymbol{\varepsilon}_{kk}$ is the volumetric strain, and $\tilde{\boldsymbol{\varepsilon}}_{ij} \equiv \boldsymbol{\varepsilon}_{ij} - \boldsymbol{\Delta}\delta_{ij}/3$ is the deviatoric strain. The 2×2 matrices $\mathbf{K}^{\mathrm{B}}$ (bulk moduli), $\boldsymbol{\mu}^{\mathrm{B}}$ (elastic moduli), $\boldsymbol{\rho}^{\mathrm{B}}$ (density) and $\mathbf{d}$ (Darcy friction) for Biot's (1956) model were given by Bourbié et al. (1987) and Morozov and Deng (2016a).

As shown by Morozov and Deng (2016a, b), inclusion of additional internal variables in model vector $\mathbf{u}$ and adding "solid viscosity" terms to function $D^{\mathrm{B}}$ leads to peaks in attenuation spectra for traveling waves similar to the well-known peak of $Q^{-1}(f)$ for the Standard Linear Solid (SLS). However, experimentally-observed attenuation and dissipation spectra typically show attenuation peaks and intervals of velocity variation that are much broader than produced by the SLS (Pimienta et al., 2015; Figure 1). Consequently, in order to explain realistic attenuation spectra together with Biot's effects, we need to extend the above model (eqs. (1)) with additional variables describing the internal deformation of the material. This can be done by using the General Linear Solid (GLS) methodology by Morozov and Deng (2016a), although with a somewhat different physical interpretation of its variables, as described below.

Let us denote the $N$ additional internal variables by a separate model vector $\boldsymbol{\theta}$, so that the dimensionality of the full GLS model is $N$+2. The components of vector $\boldsymbol{\theta}$ can include, for example, movements of various types of grain assemblages or deformations of subsets of pore volume, such as opening and closing of compliant pores containing squirt flows. However, unlike most squirt-flow models, we do not consider any micromechanical model of deformation, and the components of vector $\boldsymbol{\theta}$ remain abstract at

this point. Let us also view them as scalar quantities with respect to spatial coordinates (for example, $\theta_J$ may denote the average gap width for $J^{\text{th}}$ set of compliant pores). Further, if we also restrict ourselves to non-interacting local structures (again, such as small and sparse compliant pores or cracks containing WIFF), the Lagrangian and dissipation function should contain no spatial derivatives of local deformations ($\partial_i \boldsymbol{\theta}$). Finally, similarly to Morozov and Deng (2017), let us focus on bulk-deformation terms in eqs. (1). Considering linear and isotropic interactions, and also internal variables $\boldsymbol{\theta}$ coupled with the strain ($\boldsymbol{\Delta}$) but not the displacement of the material ($\mathbf{u}$), the most general extension of Biot's model ($L^{\text{B}}$, $D^{\text{B}}$) (equations 1) consists in additional quadratic terms containing $\boldsymbol{\theta}$ and $\dot{\boldsymbol{\theta}}$:

$$\begin{cases} L = L^{\text{B}} - \dfrac{1}{2}\boldsymbol{\theta}^T \mathbf{P}\boldsymbol{\theta} + \boldsymbol{\Delta}^T \mathbf{Q}\boldsymbol{\theta}, \\ D = D^{\text{B}} + \dfrac{1}{2}\dot{\boldsymbol{\theta}}^T \mathbf{P}'\dot{\boldsymbol{\theta}} - \dot{\boldsymbol{\Delta}}^T \mathbf{Q}'\dot{\boldsymbol{\theta}}. \end{cases} \tag{2}$$

Here, the diagonal $N\times N$ matrix $\mathbf{P}$ describes some general elastic response of the internal deformation $\boldsymbol{\theta}$, the $2\times N$ matrix $\mathbf{Q}$ describes its elastic coupling to Biot's variables, and matrices $\mathbf{P}'$ and $\mathbf{Q}'$ have similar meanings for viscosity and viscous coupling (Morozov and Deng, 2016a). In eqs. (2), we disregard any inertial effects due to the internal variables $\boldsymbol{\theta}$. The selections of signs of the coupling terms containing matrices $\mathbf{Q}$ and $\mathbf{Q}'$ will be explained later.

Note that by virtue of the generality of this formulation (Landau and Lifshitz, 1986), with appropriate choices for $N$ and the elements of matrices $\mathbf{P}$, $\mathbf{Q}$, $\mathbf{P}'$, and $\mathbf{Q}'$, eqs. (2) should give macroscopic descriptions for *all* macroscopic squirt-flow, WIFF, and other models of the rock based on mechanical principles. There exist no other reasonable combinations of the variables and their time derivatives satisfying the symmetry and linearity requirements. In the following subsection, we consider one such model, which is a rigorous extension of the concept of the Generalized SLS (GSLS) to Biot's poroelasticity. This model will be used for designing the modeling and data-fitting approach.

## Equations of Motion of Macroscopic Lagrangian Model

The equations of motion for the field $\mathbf{u}$ are obtained by taking variational derivatives of the functions $L$ and $D$ in eqs. (2) (Landau and Lifshitz, 1986). Let us write these derivatives separately for variables $\mathbf{u}$ and $\boldsymbol{\theta}$:

$$\begin{cases} \boldsymbol{\rho}\ddot{\mathbf{u}}_i = -\mathbf{d}\dot{\mathbf{u}}_i + \partial_j \boldsymbol{\sigma}_{ij}, \\ \mathbf{0} = -\mathbf{P}\boldsymbol{\theta} - \mathbf{P}'\dot{\boldsymbol{\theta}} - \mathbf{Q}^T\boldsymbol{\Delta} - \mathbf{Q}'^T\dot{\boldsymbol{\Delta}}, \end{cases} \tag{3}$$

where the Cauchy stress tensor equals:

$$\boldsymbol{\sigma}_{ij} = \mathbf{K}^{\text{B}}\boldsymbol{\Delta}\delta_{ij} + 2\boldsymbol{\mu}^{\text{B}}\tilde{\boldsymbol{\varepsilon}}_{ij} + \left(\mathbf{Q}\boldsymbol{\theta} + \mathbf{Q}'\dot{\boldsymbol{\theta}}\right)\delta_{ij}. \tag{4}$$

If we consider harmonic oscillations at angular frequency $\omega$, these relations become equations of harmonic waves in a "viscoelastic" medium with complex-valued and frequency-dependent density $\boldsymbol{\rho}^* \equiv \boldsymbol{\rho} + \dfrac{i}{\omega}\mathbf{d}$ and elasticity matrices $\mathbf{P}^* \equiv \mathbf{P} - i\omega\mathbf{P}'$ and $\mathbf{Q}^* \equiv \mathbf{Q} - i\omega\mathbf{Q}'$:

$$\begin{cases} -\omega^2 \boldsymbol{\rho}^* \mathbf{u}_i = \partial_j \boldsymbol{\sigma}_{ij}, \\ \mathbf{0} = -\mathbf{P}^*\boldsymbol{\theta} - \mathbf{Q}^{*T}\boldsymbol{\Delta}, \\ \boldsymbol{\sigma}_{ij} = \mathbf{K}^{\text{B}}\boldsymbol{\Delta}\delta_{ij} + 2\boldsymbol{\mu}^{\text{B}}\tilde{\boldsymbol{\varepsilon}}_{ij} + \mathbf{Q}^*\boldsymbol{\theta}\delta_{ij} \end{cases} \tag{5}$$

From the second eq. (5), variables $\boldsymbol{\theta}$ can be expressed through $\boldsymbol{\Delta}$:

$$\boldsymbol{\theta} = -\mathbf{P}^{*-1}\mathbf{Q}^{*T}\boldsymbol{\Delta}\,, \tag{6}$$

showing that for a massless internal structure (such as small pores containing squirt flows), its deformation is proportional to the dilatations of the rock and Biot's pore fluid. Plugging eq. 6 into 5 gives the viscoelastic stress (Morozov and Deng, 2016a):

$$\boldsymbol{\sigma}_{ij} = \mathbf{K}^{\mathrm{B}*}\boldsymbol{\Delta}\delta_{ij} + 2\boldsymbol{\mu}^{\mathrm{B}*}\tilde{\boldsymbol{\varepsilon}}_{ij}\,, \tag{7}$$

where the effective bulk modulus $\mathbf{K}^{\mathrm{B}*}$ equals

$$\mathbf{K}^{\mathrm{B}*} \equiv \mathbf{K}^{\mathrm{B}} - \mathbf{Q}^{*}\mathbf{P}^{*-1}\mathbf{Q}^{*T}\,. \tag{8}$$

Thus, by starting from the Lagrangian mechanical model given by eqs. (1) and (2),we are able to predict the effective, frequency-dependent modulus matrix $\mathbf{K}^{\mathrm{B}*}(\omega)$ that can be directly comparted to the data (Figure 1). By using this comparison, we can constrain (although non-uniquely) the mechanical parameters of the rock, as described in the next section.

## Results

In contrast to most traditional approaches to fitting attenuation data, matching some observed (drained or undrained) modulus $K(\omega)$ and the corresponding $Q^{-1}(\omega)$ is *not the only* goal of our data fitting here. In order to obtain a Biot-consistent model, we need to fit *the entire matrix* of the effective-Biot's modulus, which includes three independent parameters:

$$\mathbf{K}^{\mathrm{B}*}(\omega) = \mathbf{K}^{\mathrm{B}*}_{\mathrm{eff}}(\omega)\,. \tag{9}$$

In this paper, we only try interpreting the measurement of water-saturated Fontainebleau sandstone under the confining pressure of 1 MPa (red lines in Figure 1). By taking $N = 3$, using the drained compliance $K_D^{-1}$ shown in Figure 1 and constant fluid ($K_f = 2.25$ GPa) and solid-grains moduli ($K_s = 37$ GPa) and varying the mechanical matrices $\mathbf{K}^{\mathrm{B}}$, $\mathbf{Q}$, $\mathbf{P}$, $\mathbf{Q}'$ and $\mathbf{P}'$ , the bulk modulus $\mathbf{K}^{\mathrm{B}*}_{\mathrm{eff}}(\omega)$ is predicted to match the data, as shown by black lines in Figure 2. The inverted mechanical properties of the rock are shown in Table 1.

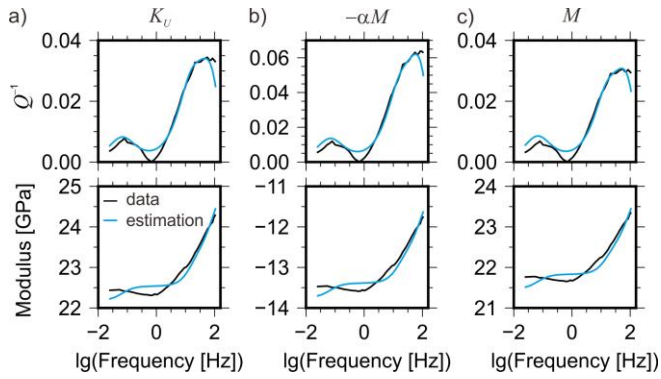


Figure 2. Interpreted physical quantities of laboratory measurements on water-saturated Fontainebleau sandstone under pressure 1 MPa. $K_U$, $\alpha M$ and $M$ are Biot's moduli.

The inverted model (Table 1) is useful in several ways. First, most importantly, this model gives a rigorous, purely mechanical system providing a good fit to the experimental results and directly relating the experimental measurements to physical properties. This model clearly shows that the rock does not need to have "material memory" or frequency-dependent properties in order to account for the observations in close detail. Some parts of the observed spectra at low-frequencies are not perfectly fit, and the mechanical model shows that such intervals of negative dispersion actually cannot be explained by linear mechanical models. Such intervals of negative dispersion may be related to the effects of the experimental setup, such as "dead volume" at the ends of the sample (Pimienta et al., 2016), or to other types of experimental errors. Second, the variations of the inverted moduli and particularly viscosities (Table 1) represent quantitative measures of the mechanical structure of the sandstone specimen. This mechanical structure can be directly utilized to implement numerical modeling of any types of deformations and waves by using eqs. (5).

## Conclusions

A Biot-consistent, Lagrangian, macroscopic model is formulated and used to interpret low-frequency laboratory data for attenuation and dispersion in fluid-saturated sandstone. This model reveals the true, frequency- and time-dependent mechanical properties of the material. This model can readily be used for modeling any experiments in the laboratory and in the field.

Table 1. Model parameters for water-saturated sandstone at pressure 1MPa

| $\mathbf{K}^B$ (GPa) | | | | |
|---|---|---|---|---|
| $\mathbf{K}^B(1,1)$ | | $\mathbf{K}^B(1,2)$, $\mathbf{K}^B(2,1)$ | $\mathbf{K}^B(2,2)$ | ($i$, $j$) indicates $i^{th}$ row and $j^{th}$ column of a matrix |
| 27.26 | | -9.01 | 25.89 | |
| **Elasticity (GPa)** | | | | |
| $J$ | 1 | 2 | 3 | Index of the column |
| $Q_{1J}$ | 3.75 | 6.00 | 10.92 | First row of **Q** matrix |
| $Q_{2J}$ | 3.76 | 5.43 | 10.19 | Second row of **Q** matrix |
| $P_{JJ}$ | 38.93 | 37.39 | 31.69 | Diagonal of **P** matrix |
| **Viscosity (MPa·s)** | | | | |
| $Q'_{1J}$ | 26.80 | 0.22 | 5.62 | First row of **Q′** matrix |
| $Q'_{2J}$ | 0.02 | 0.39 | 5.16 | Second row of **Q′** matrix |
| $P'_{JJ}$ | $9.27\times10^4$ | 373.90 | 52.17 | Diagonal of **P′** matrix |

## Acknowledgements

This research was supported by Discovery grant RGPIN 05408-2016 from Natural Sciences and Engineering Research Council (Canada). Plots are produced using Generic Mapping Tools (http://gmt.soest.hawaii.edu/).

### References

Chapman, M., S. V. Zatcepin, and S. Crampin, 2002. Derivation of a microstructural poroelastic model: Geophys. J. International, 151, 427–451.

Deng, W., and I. B. Morozov, 2016, Solid viscosity of fluid-saturated porous rock with squirt flows at seismic frequencies: Geophysics, 81, no. 4, D395-D404.

Biot, M. A. 1956, Theory of propagation of elastic waves in a fluid-saturated porous solid. I. Low-frequency range: The Journal of the Acoustical Society of America, 28, no. 2,168-178.

Bourbié, T., O. Coussy, and B. Zinszner. 1987, Acoustics of porous media: Editions Technip. Paris, France.

Landau, L., and E. Lifshitz. 1986, Course of theoretical physics, volume 7 (3rd English edition): Theory of elasticity: Butterworth-Heinemann, ISBN 978-0-7506-2633-0.

Gurevich, B., D. Makarynska, O. B. de Paula, and M. Pervukhina, 2010, A simple model for squirt-flow dispersion and attenuation in fluid-saturated granular rocks: Geophysics, 75, no. 6, N109–N120.

Morozov, I. B., and W. Deng. 2016a, Macroscopic framework for viscoelasticity, poroelasticity, and wave-induced fluid flows—Part 1: General linear solid: Geophysics, 81, no. 1, L1–L13.

———————— 2016b, Macroscopic framework for viscoelasticity, poroelasticity, and wave-induced fluid flows—Part 2: Effective media: Geophysics, 81, no. 4, D405–D417.

————————2017, Inversion for Biot-consistent material properties in subresonant oscillation experiments with fluid-saturated porous rock: Geophysics, doi: 10.1190/geo2017-0511.1

Müller, T. M., B. Gurevich, and M. Lebedev, 2010, Seismic wave attenuation and dispersion resulting from wave-induced flow in porous rocks—A review: Geophysics, 75, no. 5, 75A147-175A164.

Pimienta, L., J. Fortin, and Y. Guéguen, 2015, Young modulus dispersion and attenuation in sandstones: Geophysics 80, no. 5, L57–L72, doi:10.1190/GEO2014-0532.1.

Pimienta, L., J.V.M. Borgomano, J. Fortin, and Y. Guéguen, 2016, Modelling the drained/undrained transition: effect of the measuring method and the boundary conditions: Geophysical Prospecting, 64, 1098–1111, doi: 10.1111/1365-2478.12390